PFC/JA-89-21

An Electrostatic Barrier Scrape-off Layer as a Technique to Reduce Impurity Sources from Plasma Bombardment of RF Antenna Structures

LaBombard, B.

Plasma Fusion Center
Massachusetts Institute of Technology
Cambridge, MA 02139

March 1989

Submitted to: Nuclear Fusion

This work was supported by the U. S. Department of Energy Contract No. DE-AC02-78ET51013. Reproduction, translation, publication, use and disposal, in whole or in part by or for the United States government is permitted.

Table of Contents

An Electrostatic Barrier Scrape-off Layer as a Technique to Reduce Impurity Sources from Plasma Bombardment of RF Antenna Structures

B. LaBombard

Plasma Fusion Center
Massachusetts Institute of Technology
167 Albany St.
Cambridge, MA 02139 USA

A new technique is proposed that may allow one to reduce the bombarding flux of plasma onto critical RF antenna components (Faraday shield) yet maintain a high plasma density relatively near the antenna to maximize coupling efficiency. The scheme principally involves the formation a mobility limited transport layer or "Electrostatic Barrier Scrape-off Layer" (EBSOL) to inhibit locally the cross-field flux of ions onto plasma-facing structures. Limiters which are normally employed to protect the Faraday shield from direct plasma contact are modified and biased electrically positive, forming a narrow boundary layer plasma in front of the Faraday shield with a significantly reduced density e-folding length.

A simplified two fluid transport model which includes phenomenological cross-field diffusion and mobility is used to estimate the effect of the EBSOL on the local density e-folding length. The model predicts that the influence of an applied bias on the local density e-folding length depends only on the relative magnitudes of cross-field ion and electron mobilities. Thus, even in the case of anomalous diffusion (Bohm) and classical cross-field mobility, characteristic density e-folding lengths in front of the Faraday shield may be reduced by up to a factor of five with positive bias potentials on the order of three times the local electron temperature. The result is independent of the magnetic field strength, and suggests that an order of magnitude or more reduction in the ion sputtering rate on the Faraday shield may be achievable. The result also suggests that cross-field mobility may play an important role in scrape-off layer transport even in the absence of an externally imposed bias - an effect that is typically overlooked in tokamak scrape-off layer transport analysis.

As a specific example of the EBSOL technique, an arrangement that might be employed to protect the Faraday shield of an Alcator C-MOD ICRF antenna structure is considered. Bias potentials, currents, heat fluxes, and reduced densities at the Faraday shield are estimated for anticipated plasma conditions. The dimensionless phenomenological transport parameter Λ ($= T\,\mu_\perp/D_\perp$) is shown to be important for assessing the practical viability of the EBSOL technique, with $\Lambda << 1$ implying that multiple biased limiter electrodes in minor radius may be required. A need is identified for experimental characterizations of the role of cross-field mobility in the near fully ionized, turbulent scrape-off layer plasmas of tokamaks.

1. INTRODUCTION

It is recognized that impurity sources from RF antenna structures can result from a variety of interactions between the plasma in the vicinity of the surface, the RF fields, and the surface itself [1-5]. Neutral gas generated by plasma recombination on antenna surfaces and/or desorption may also play a role through RF breakdown and ionization. Obviously, the most effective way to reduce the impurity generation rate is to minimize the plasma density at all antenna surfaces. However, given that the scrape-off density profile is relatively fixed (by Bohm diffusion for example), one may not minimize the plasma density at the antenna surface while maximizing the plasma density near the antenna for improved coupling efficiency. In order to meet these two competing goals, an independent means for controlling the cross-field particle transport near the antenna is desirable.

Experiments have shown that cross-field transport in a tokamak scrape-off layer plasma can be significantly altered by externally imposing an electrical potential to limiter and/or wall surfaces [6-11]. These "biased scrape-off layer" experiments typically exhibit a modified density e-folding length that is longer or shorter than the "unperturbed" value, depending on the polarity of the applied potential. The mechanism responsible for the local reduction or enhancement in the cross-field particle flux can be viewed qualitatively as a formation of a "electrostatic barrier" to cross-field ion flow. It has been suggested that such electrostatic barrier scrape-off layers (EBSOLs) may be used to control the distribution of plasma fluxes to divertor and/or limiter structures at the plasma edge [12].

This paper examines the use of an EBSOL specifically as a technique for plasma density profile control near a RF antenna structure. It is suggested that an EBSOL is relatively easy to form for an RF antenna and may provide a crucial means of reducing plasma sputtering on antenna surfaces. The ability to dynamically control the plasma density at a given surface is also useful from the point of view of assessing that surface's contribution to the total impurity source strength.

A simplified non-ambipolar transport model for a biased scrape-off layer plasma is presented in section 2. Cross-field ion and electron transport in a turbulent plasma scrape-off layer is assumed to be governed by phenomenological coefficients of diffusion and mobility. The model yields a rough estimate of the local density e-folding length modification that may be achieved when an electrical bias is applied. Section 3 outlines a method for implementing an EBSOL to reduce the plasma density on an antenna's Faraday shield. Graphs of local density e-folding length reduction, density reduction (at the Faraday shield), total bias current, and increase in peak surface power flux that correspond to an applied bias voltage are assembled using the transport model. As an example case, bias currents, voltages, and reduced densities at the Faraday shield are estimated for an EBSOL that could

be used in an RF antenna structure for the Alcator C-Mod tokamak. Section 4 discusses some assumptions that are used in estimating the density profile from the transport model and the conditions for their validity. It is pointed out that the sensitivity of the cross-field density profile on the local wall potential (as predicted from the simplified non-ambipolar transport model) suggests that one should generally include non-ambipolar transport effects when analyzing scrape-off layer transport. The need for more systematic measurements of plasma potential profiles in scrape-off layers and for detailed experimentation on cross-field transport in fully ionized, turbulent boundary layer plasmas is emphasized by this work. Section 5 summaries the contents of this paper.

2. A SIMPLE NON-AMBIPOLAR TRANSPORT MODEL FOR AN ELECTROSTATIC BARRIER SCRAPE-OFF LAYER (EBSOL)

In order to estimate the influence of biased wall surfaces on the cross-field transport in a scrape-off layer, one needs to develop a model that includes non-ambipolar transport. The model presented here closely follows the one discussed in reference [13]. It is a relatively simple model that is based on the assumption that the cross-field electron and ion fluxes in a turbulent scrape-off layer can be written in terms of phenomenological coefficients of diffusion ($D_\perp$) and mobility ($\mu_\perp$). The model is similar in many ways to the classic plasma physics problem of Simon [14] who considered cross-field transport in a magnetized plasma column when the magnetic field lines terminate on conducting walls.

Consider the geometry of a biased scrape-off layer (BSOL) shown in Fig. 1. The BSOL is bounded along field lines running parallel to the z axis by limiters, divertor plates, or some other wall surfaces spaced at a distance of 2L. The interface between the main plasma and BSOL occurs on the z axis at r=a and it is assumed that no gradients exist in the $\mathbf{B}\times\hat{\mathbf{r}}$ direction. The limiters are held fixed at some potential, Φ_w, which may be different than the local floating potential, Φ_f.

The BSOL is populated by a cross-field plasma flux ($\Gamma_\perp = \Gamma_r$) from the main plasma region and depleted by a parallel plasma flux ($\Gamma_{//} = \Gamma_z$) flowing to limiter/divertor surfaces. For simplicity, neutral densities in the BSOL are assumed to be low enough so that ionization can be neglected in the particle balance. This assumption is justified for the short connection lengths (L) that would exist in an EBSOL designed for an RF antenna structure. Analogous to the particle flux, a cross-field plasma current ($\mathbf{J}_\perp$) is assumed to flow from the main plasma into the BSOL while a parallel plasma current ($\mathbf{J}_{//}$) flows to limiter surfaces (independent of the equilibrium plasma currents that exist in the core plasma).

In the presheath plasma zone, the density and potential varies by a factor of ~2 and ~0.5 T_e respectively along the magnetic field. (This paper defines all

temperatures in units of eV so that Boltzmann's constant, κ, is defined as $\kappa = q$.) In contrast, the density may vary by orders of magnitude in the cross-field direction. The model developed here will focus on the cross-field variation of the density and potential by considering a spatial average of these quantities along the magnetic field. Since the Debye length is negligible compared to the connection length, a spatial average of plasma parameters will be performed over the entire BSOL region between $z=-L$ and $z=L$.

2.1 Radial Fluxes and Currents

Radial transport of electrons and ions are modelled by

$$\Gamma_r^e = -D_\perp^e \nabla_r n - \mu_\perp^e n \mathbf{E}_r \tag{1}$$

$$\Gamma_r^i = -D_\perp^i \nabla_r n + \mu_\perp^i n \mathbf{E}_r \tag{2}$$

where $D_\perp$ is typically on the order of Bohm diffusion and assumed to be governed by plasma turbulence. If the turbulence is due to low frequency electrostatic fluctuations, one expects that $D_\perp$ would be approximately equal for ions and electrons. However, it is not clear what the effective values for $\mu_\perp$ are in a turbulent plasma, or if $\mu_\perp$ itself is dependent on $\mathbf{E}_r$. As a lower bound, one may assume that $\mu_\perp^i$ and $\mu_\perp^e$ are determined classically from ion-neutral and electron-neutral collisions. In any event, this analysis can be generalized to include anomalous values of all coefficients.

From Eqs. (1) and (2), the radial plasma flux and current are

$$\Gamma_r = -D_\perp^i \nabla_r n + \mu_\perp^i n \mathbf{E}_r \tag{3}$$

$$\frac{\mathbf{J}_r}{q} = -(D_\perp^i - D_\perp^e) \nabla_r n + (\mu_\perp^i + \mu_\perp^e) n \mathbf{E}_r . \tag{4}$$

In steady state, with no particle sources in the BSOL,

$$\nabla_r \cdot \Gamma_r = -\nabla_{//} \cdot \Gamma_{//} \tag{5}$$

$$\nabla_r \cdot \mathbf{J}_r = -\nabla_{//} \cdot \mathbf{J}_{//} \tag{6}$$

and averaging Eqs. (5) and (6) over z=-L to z=L yields

$$\nabla_r \cdot \overline{\Gamma_r} = -\frac{\Gamma^w_{//}}{L} \tag{7}$$

$$\nabla_r \cdot \overline{\mathbf{J}_r} = -\frac{J^w_{//}}{qL} \tag{8}$$

where $\Gamma^w_{//}$ and $J^w_{//}$ are the parallel flux and current at the limiter surface. Averaging Eqs. (3) and (4) from z=-L to z=L and using Eqs. (7) and (8) yields

$$-D^i_\perp \nabla_r^2 \overline{n} + \mu^i_\perp \nabla_r \cdot \overline{n\,\mathbf{E}_r} = -\frac{\Gamma^w_{//}}{L} \tag{9}$$

$$-(D^i_\perp - D^e_\perp)\nabla_r^2 \overline{n} + (\mu^i_\perp + \mu^e_\perp)\nabla_r \cdot \overline{n\,\mathbf{E}_r} = -\frac{J^w_{//}}{qL} . \tag{10}$$

For simplicity, the transport coefficients have been assumed to be independent of space (or explicitly, n and $\mathbf{E}_r$). Eliminating the $\overline{n\,\mathbf{E}_r}$ terms by combining Eqs. (9) and (10) results in

$$(D^i_\perp \mu^e_\perp + D^e_\perp \mu^i_\perp)\nabla_r^2 n = (\mu^i_\perp + \mu^e_\perp)\frac{\Gamma^w_{//}}{L} - \mu^i_\perp \frac{J^w_{//}}{qL} . \tag{11}$$

and similarly eliminating $\nabla_r^2 \overline{n}$ terms in Eqs. (9) and (10) yields

$$(D^i_\perp \mu^e_\perp + D^e_\perp \mu^i_\perp)\nabla_r \cdot n\nabla_r\Phi = (D^e_\perp - D^i_\perp)\frac{\Gamma^w_{//}}{L} + D^i_\perp \frac{J^w_{//}}{qL} \tag{12}$$

where $\mathbf{E}_r = -\nabla_r\Phi$.

The overbar notation that indicated an averaging operation along z in Eqs. (7)-(11) has been dropped in Eqs. (11) and (12). However, all quantities should be taken to represent a spatial average over the presheath variation here and for the remainder of this paper. Equation (12) makes use of an additional assumption that $\overline{n \mathbf{E}_r} \approx \bar{n} \bar{\mathbf{E}}_r$.

2.2 Parallel Fluxes and Currents

Along the magnetic field, presheath electric fields draw ions to the limiter surfaces so as to satisfy the Bohm sheath condition. This situation persists under a wide range of limiter biases as long as the local limiter potential remains approximately 0.5 T_e below the plasma potential at z=0. Thus the parallel plasma flux to the wall can be modelled as

$$\Gamma_{//}^{w} = \alpha n C_s \tag{13}$$

where α is a parameter in the range $0.5 < \alpha < 1$, and C_s is the ion sound speed.

The parallel plasma current to the wall can be estimated from planar Langmuir probe theory. Given the same restriction on wall potential mentioned above,

$$J_{//}^{w} = \alpha q n C_s\left[1 - \exp\left(\frac{\Phi_w - \Phi_f}{T_e}\right)\right] . \tag{14}$$

By defining the plasma potential at the sheath edge to be zero, Eq. (14) approximately applies for $-\infty < \Phi_w < 0$. (Note that Φ_f is a negative quantity.)

2.3 Radial Density and Potential Profiles in a Biased Scrape-off Layer

Combining Eqs. (13) and (14) with (11) and (12) results in an equation for the density profile in the BSOL,

$$L\left(D_{\perp}^{i}\mu_{\perp}^{e} + D_{\perp}^{e}\mu_{\perp}^{i}\right) \nabla_r^2 n = \alpha n C_s\left[\mu_{\perp}^{e} + \mu_{\perp}^{i} \exp\left(\frac{\Phi_w - \Phi_f}{T_e}\right)\right] , \tag{15}$$

and an equation for the potential profile,

$$L\,(D_\perp^i \mu_\perp^e + D_\perp^e \mu_\perp^i)\,\nabla_r \cdot n \nabla_r \Phi \;=\; \alpha\, n\, C_s \left[D_\perp^e \;-\; D_\perp^i \exp\left(\frac{\Phi_w - \Phi_f}{T_e}\right)\right] \;, \qquad (16)$$

for a prescribed wall potential profile. Note that Φ_f is in general coupled to Φ (through T_e for example).

Equations (15) and (16) form a pair of coupled nonlinear second order differential equations for n and Φ which can not be integrated analytically for the arbitrary functions $\Phi_w(r)$ and $\Phi_f(r)$. However, consider the case when the limiter surface is biased in such a way as to hold $(\Phi_w - \Phi_f)/T_e$ constant in r. (This condition may be satisfied by looking at a restricted set of Φ_w and/or T_e profiles.) In this case, the density profile that solves Eq. (15) and meets the boundary condition of zero density as $r \to \infty$ is simply

$$n(r) \;=\; n_0 \, \exp(-r/\lambda) \qquad (17)$$

where

$$D_\perp^* \;=\; D_\perp \, f(\Phi_w) \qquad (18)$$

$$\lambda \;=\; \sqrt{\frac{D_\perp^* \, L}{\alpha \, C_s}} \qquad (19)$$

and

$$f(\Phi_w) \;=\; \frac{\mu_\perp^e \;+\; \mu_\perp^i}{\mu_\perp^e + \mu_\perp^i \exp\left(\frac{\Phi_w - \Phi_f}{T_e}\right)} \qquad (20)$$

and it has been assumed that $D_\perp^e = D_\perp^i = D_\perp$.

In the case of a non-conducting or locally floating limiter, Eqs. (17)-(20) yield $f(\Phi_w) = 1$, $D_\perp^* = D_\perp$, and the density profile has an e-folding length that is related to $D_\perp$ through the familiar relationship

$$D_\perp \;=\; \frac{\alpha \, \lambda_0^2 \, C_s}{L} \;. \qquad (21)$$

For later reference, the scrape-off length for this case of a locally floating limiter is denoted by λ_0.

Similarly, the potential profile that solves Eq. (16) and remains bounded as r $\rightarrow \infty$ is

$$\Phi(r) = - \frac{D_\perp^* \left[1-\exp\left(\frac{\Phi_w-\Phi_f}{T_e}\right)\right] r}{(\mu_\perp^e + \mu_\perp^i)\,\lambda} + \Phi_0 . \qquad (22)$$

Again, it should be pointed out that the above results apply only to the case when the quantity $(\Phi_w-\Phi_f)/T_e$ is independent of r. This is actually quite restrictive. In general, a biased scrape-off layer may have radial potential and temperature profiles that are somewhat arbitrary. A metallic limiter, even though it is not actively biased, will effectively impose a positive bias at some radial locations and a negative bias at other radial locations. Furthermore, the assumption that $D_\perp^e = D_\perp^i = D_\perp$ may only be approximately true. For example, if cross field "diffusion" results from low frequency electrostatic turbulence plus ion-neutral, electron-neutral and ion-electron collisions, one might expect that the quantity $D_\perp^i - D_\perp^e$ would be positive and approximately equal to the ion diffusion rate from ion-neutral collisions. In this case, Eq. (22) would be modified and would predict a radial electric field even in the absence of an applied bias ($\Phi_w = \Phi_f$). Nevertheless, within the restrictions implicit in Eqs. (17)-(22), one can make some simple quantitative estimates of the effect of an applied bias on density profiles in a BSOL.

Equations (17)-(20) predict that the density e-folding length will increase for negative limiter biases and decrease for positive limiter biases (relative to the local floating potential). It is important to note that this model predicts a significant modification to the local density e-folding length, independent of the magnitudes of $\mu_\perp^e$ and $\mu_\perp^i$ relative to $D_\perp$. Since no explicit relationship (e.g. Einstein relation) was postulated between the phenomenological mobility and diffusion coefficients in deriving Eqs. (17)-(22) an interesting situation arises: Although the value of $D_\perp$ determines the overall spatial scale of the density e-folding length, even a slight amount of cross-field mobility (classical mobility from neutral collisions, for example) may allow one to greatly modify the local density e-folding length through an electrical bias. Given that the edge plasma is strongly turbulent, it is difficult to estimate the appropriate phenomenological values for $\mu_\perp^e$ and $\mu_\perp^i$. Nevertheless, consider the following three scenarios: (a) $\mu_\perp^i >> \mu_\perp^e$, (b) $\mu_\perp^i \approx \mu_\perp^e$, and (c) $\mu_\perp^i << \mu_\perp^e$.

A. $\mu_\perp^i >> \mu_\perp^e$

If one assumes that the electron and ion mobilities are classical and determined by neutral collisions, then $\mu_\perp^i/\mu_\perp^e \sim m_i/m_e$ when the electron-neutral and ion-neutral collision frequencies are comparable. Even when accounting for an order of magnitude higher frequency of electron-neutral collisions in the SOL plasma, $\mu_\perp^e$ can be safely neglected relative to $\mu_\perp^i$ (as long as $\Phi_w - \Phi_f \gtrsim -T_e \ln[\mu_\perp^i/\mu_\perp^e]$) so that Eq. (20) becomes

$$f(\Phi_w) \approx \exp\left(\frac{\Phi_f - \Phi_w}{T_e}\right) . \tag{23}$$

Consequently, the density e-folding length due to an applied bias is simply

$$\lambda \approx \exp\left(\frac{\Phi_f - \Phi_w}{2T_e}\right) \lambda_0 . \tag{24}$$

This case yields the most dramatic change in the local density scrape-off length for a given bias. Modified e-folding lengths in the range $0.22 < \lambda/\lambda_0 < 4.5$ are attainable for plasma with $\Phi_f \approx -3\ T_e$ and $-6\ T_e \le \Phi_w \le 0$. It is important to note that the local modification in density e-folding length predicted by Eq. (24) is <u>independent</u> of the magnetic field strength, the cross-field diffusion coefficient, and the mechanisms that determine the phenomenological values for $\mu_\perp^i$ and $\mu_\perp^e$. All that is required is $\mu_\perp^i >> \mu_\perp^e$. It may also be noted that an impurity species with mass $m_z >> m_i$ can similarly yield $\mu_\perp^z >> \mu_\perp^i$, implying that impurity density profiles may be most sensitive to radial electric fields.

B. $\mu_\perp^i \approx \mu_\perp^e$

It is possible to imagine situations where the perpendicular electron mobility is strongly enhanced by parallel electron transport through electromagnetic turbulence or by an ergodic magnetic field structure in the SOL plasma. If $\mu_\perp^e$ becomes comparable to $\mu_\perp^i$, the density e-folding length is,

$$\lambda \approx \lambda_0 \sqrt{\frac{2}{1 + \exp\left(\frac{\Phi_w - \Phi_f}{T_e}\right)}} . \tag{25}$$

The scrape-off length modification accessible to the BSOL is then $0.31 < \lambda/\lambda_0 < 1.4$ for plasma with $\Phi_f \approx -3\ T_e$ and $-6\ T_e \leq \Phi_w \leq 0$.

C. $\mu_\perp^i << \mu_\perp^e$

In this extreme limit, limiter bias has no effect on the density profile and the e-folding length is fixed at $\lambda \approx \lambda_0$.

3. AN EBSOL AS A TECHNIQUE TO REDUCE PLASMA BOMBARDMENT ON AN ANTENNA'S FARADAY SHIELD

3.1 Geometry of Antenna, Bias Limiters, and EBSOL

Figure 2 shows conceptually how an EBSOL might be formed to reduce plasma bombardment of an RF antenna's Faraday shield. Most antenna structures employ a pair of limiters which protect the Faraday shield from direct contact with plasma streaming along magnetic field lines. The technique proposed here is to modify segments of these limiters such that they can be biased positive with respect to the local floating potential. As shown in Fig. 2, only segments of the limiter which intercept magnetic field lines passing in front of the Faraday shield need be biased. The limiter segments may consist of a single "electrode" (as shown in Fig. 2) or a series of independently biased electrodes spanning the radial distance, δ. The latter configuration would allow some control of $\Phi_w(r)$ and therefore the radial variation of $(\Phi_w-\Phi_f)/T_e$, although it adds some undesirable complexity. (For the sake of simplifying the analysis, $(\Phi_w-\Phi_f)/T_e$ will be assumed to be established independent of radius so that the results in section 2 can be used throughout the radial distance, δ. Conditions for the validity of this assumption are discussed in section 4.)

The positive bias should be referenced with respect to a plasma-facing surface that has a large "wetted area" relative to the biased limiter segments, i.e., one that receives a large ion flux from the plasma core such as a primary limiter or a divertor neutralizer plate (or the vacuum vessel wall if it is electrically connected to either of these). In this way, most of the bias voltage will appear as a finite value of $\Phi_w-\Phi_f$ in the EBSOL and not merely as a change in the sheath potential drop at the negatively biased reference surface. This condition on the ratio of "wetted areas" will be satisfied if the total ion current to the reference surface is about 100 times the total ion current to the limiter segments without bias. (The "electron saturation" flux is typically on the order of 20 times the "ion saturation" flux to a biased object.)

Biasing the entire limiter structure that surrounds the Faraday shield may achieve the same effect. However, it would unnecessarily require a much larger bias current, particularly since a direct electrical connection might exist along magnetic field lines to the reference limiter or divertor surfaces. This technique may also be less effective in producing a positive plasma potential perturbation in front of the Faraday shield since in some cases an appropriately large ratio of "wetted areas" may be more difficult to achieve. (Biasing the Faraday shield itself may be impractical since RF fields cause portions of the shield to "oscillate" at kV potentials.)

3.2 EBSOL Voltage, Current, and Peak Heat Flux

A. Bias Voltage

The goal is to reduce the plasma density at the surface of the Faraday shield. The cross-field density profile, $n(r)$, in front of the Faraday shield may be approximated by Eqs. (17)-(20) with $2L$ being the distance between the biased limiter surfaces along field lines. Denote the distance that the Faraday shield is recessed behind the leading edge of the limiters as δ. For the case of no applied bias, the plasma density at the Faraday shield, n_{F0}, can be written in terms of the density at the leading edge of the biased limiters, n_0, as approximately

$$n_{F0} \approx n_0 \exp(-\delta/\lambda_0) \tag{26}$$

where λ_0 is determined by Eq. (21). With an electrical bias, the density at the Faraday shield is reduced to the value

$$n_F \approx n_0 \exp(-\delta/\lambda) = n_{F0} \exp[(-\delta/\lambda_0)(\lambda_0/\lambda - 1)] . \tag{27}$$

Figure 3 plots n_F/n_{F0} for various values of δ/λ_0 versus the normalized bias potential, $(\Phi_W-\Phi_f)/T_e$. Figure 3(a) considers the case of $\mu_\perp^i >> \mu_\perp^e$ while Fig. 3(b) considers $\mu_\perp^i = \mu_\perp^e$. The quantity λ/λ_0 that was used in evaluating Eq. (27) is also plotted in Fig. 3. This figure clearly shows that an order of magnitude or more reduction in the plasma density at the Faraday shield may be achievable by the EBSOL technique.

Biases with $\Phi_W > 0$ could, in principle, yield an even further reduction in the density at the Faraday shield. However, beyond the limit of $\Phi_W \approx 0$ the model used here breaks down. Equations (13) and (14) would need to be modified in order to account for the "inverted" presheath electric field that can result with $\Phi_W > 0$. Of course the density e-folding length cannot be made infinitesimally small since a

finite plasma density is needed to support the electron current that must flow to the biased limiter surfaces. In addition, quasineutrality constrains the density e-folding length to be larger than a characteristic ion Larmor radius, $\lambda \gtrsim \rho_i$. In any event, the maximum available bias current and/or the maximum allowable heat flux to the biased surface typically restricts the bias to be $\Phi_w < 0$, for most cases of interest. (Recall that the value of plasma potential at the sheath edge is defined to be zero.)

B. Bias Current

The current through the external power supply can be obtained by integrating Eq. (14) over the biased limiter segments. The model yields an approximate value for the net current collected by all biased limiter segments, I_b, of

$$I_b \approx 2 \alpha q n_0 C_s \lambda w \{\exp[(\Phi_w - \Phi_f)/T_e] - 1\} , \qquad (28)$$

assuming that $\delta/\lambda >> 1$. The parameter, w, is the width of the biased limiter segments in the poloidal ($\sim \mathbf{B} \times \hat{\mathbf{r}}$) direction.

Figure 4 plots a normalized value of I_b versus normalized bias potential for the two cases of $\mu_\perp^i >> \mu_\perp^e$ and $\mu_\perp^i = \mu_\perp^e$. To obtain I_b in the units of amps, multiply the right hand ordinate in Fig. 4 by the quantity, $\alpha n_{14} \lambda_0 w T_e^{1/2}$, where λ_0 and w have the units of cm, T_e the units of eV, and n_{14} the units of 10^{14} cm^{-3}. For the purposes of evaluating the sound speed, it has been assumed that $T_i \approx T_e$ and $C_s^2 = q(T_i + T_e)/m_{H^+}$.

C. Peak Power Flux to a Positively Biased Limiter

At large positive biases, the electron heat flux to the limiter surface can greatly increase. The maximum heat flux that a biased surface can withstand ultimately determines the maximum positive bias potential that can be applied at high plasma densities. An estimate of the plasma heat flux to a positively biased limiter surface is therefore needed.

In general, the plasma power flux to a surface depends on a variety of plasma and surface parameters. The dominant parameters are the ion temperature, electron temperature, ion mass, secondary electron emission coefficient (γ_{se}), and electrical bias voltage [15]. The peak power flux (P_p) flowing along magnetic field lines to the biased limiter surface at r=0 can be written as

$$P_P \approx \alpha\, q\, n_0\, C_s\, T_e \{ -(\Phi_w - \Phi_f)/T_e - 0.5\, \mathrm{Ln}[(1+T_i/T_e)(2\pi\, m_e/m_i)] + \mathrm{Ln}(1-\gamma_{se}) + 2\, T_i/T_e + 2\, \exp[(\Phi_w - \Phi_f)/T_e]/(1-\gamma_{se}) \} . \quad (29)$$

Figure 4 plots a normalized value of P_P versus normalized bias potential for the case of $T_i = T_e$ and $m_i = m_{H^+}$. To obtain P_P in the units of watts/cm^2, multiply the left hand ordinate in Fig. 4 by the quantity, $\alpha\, n_{14}\, T_e^{3/2}$. Figure 4 shows that a factor of 6 to 10 increase in the peak limiter heat flux must be accommodated for the case of a strong positive bias, $(\Phi_w - \Phi_f)/T_e \approx 3$. A more moderate bias of $(\Phi_w - \Phi_f)/T_e \approx 1.5$ yields a factor of 2 to 3 increase in heat flux. Such heat fluxes many be accommodated by shaping the biased limiter segments to spread the heat load over a larger surface area. (This is in contrast to the biased limiter segments shown in Fig. 2 which indicate no "shaping").

It should be noted that the ion sputtering rate on the leading edge of the biased limiter segments may be reduced, although this is not the primary motivation for applying the positive bias. An impurity species with charge Z strikes the biased limiter surface with an energy that is reduced by $Z(\Phi_w - \Phi_f)$. The ion impact energy may consequently be lowered below the sputtering threshold for many impurities.

3.3 Parameters for an EBSOL in a C-MOD RF Antenna Structure

Table 1 shows estimates of plasma density reduction at a Faraday shield and corresponding bias currents and peak power fluxes for an EBSOL operating in the Alcator C-MOD Tokamak. The values shown are "conservative" in that they are based on a case with a relatively high density at the leading edge of the biased limiter segments (5×10^{13} cm^{-3}). The edge plasma conditions show in Table 1 are scaled from SOL measurements made in high density, high magnetic field plasmas on the Alcator C Tokamak [16]. Table 1 suggests that an order of magnitude reduction of the plasma flux bombarding the Faraday shield may be possible for reasonable values of bias voltage, current, and increased peak power flux.

4. DISCUSSION

4.1 Validity of Assumption that $(\Phi_w-\Phi_f)/T_e \approx$ constant

An important assumption used in the above analysis is that the limiters can be biased in such a way as to hold $(\Phi_w-\Phi_f)/T_e \approx$ constant in radius, independent of the profiles of $\Phi(r)$ and $T_e(r)$ (quantities which also are functions of wall bias). Clearly, by segmenting the limiters into a sufficient number of independently biased electrodes at various radii, this assumption can be met by suitably adjusting the wall potential profile (with exception to the singular case when $\mu_\perp^i = \mu_\perp^e = 0$ and an infinite radial electric field is allowed to exist). However, the need for a large number of electrodes makes implementation of the EBSOL scheme impractical. Alternatively, a very strong positive bias may be applied to a single electrode such that one attempts to achieve $(\Phi_w-\Phi_f)/T_e \gtrsim$ 1-2 throughout the entire scrape-off zone. In this case, the results in section 3 could be used to estimate the minimum density reduction at the Faraday shield. Unfortunately, this technique may also lead to unacceptably high heat fluxes at the biased limiter's leading edge. The conditions under which multiple electrodes must be used to meet the assumption of $(\Phi_w-\Phi_f)/T_e \approx$ constant is therefore of interest.

The local floating potential can be approximated as $\Phi_f(r) \approx -\beta\, T_e(r) + \Phi(r)$, where $\beta \sim 3$ for hydrogen plasmas. The change in the quantity $(\Phi_w-\Phi_f)/T_e$ over the radial extent of an electrode biased at a uniform potential, Φ_w, can be estimated from

$$\Delta\left(\frac{\Phi_w-\Phi_f}{T_e}\right) \approx -\frac{\Delta\Phi}{T_e} - \left(\frac{\Phi_w-\Phi_f}{T_e}\right)\frac{\Delta T_e}{T_e} \qquad (30)$$

where $\Delta\Phi$ and ΔT_e are the corresponding changes in plasma potential and electron temperature over the radial extent of the electrode. For biases of interest, the quantity $(\Phi_w-\Phi_f)/T_e$ is positive and of order unity. The electron temperature generally decreases with increasing radius, while Eq. (22) shows that the plasma potential increases with increasing radius at a rate that depends on the ratio $D_\perp/\mu_\perp$. (In the more general case when $D_\perp^e \neq D_\perp^i$, positive wall bias causes the potential to increase in radius relative to its no-bias profile.) These two effects may compensate somewhat to hold $(\Phi_w-\Phi_f)/T_e \approx$ constant. However, a large variation in $(\Phi_w-\Phi_f)/T_e$ may occur over the electrode when $\Delta T_e \approx 0$ and the ratio $D_\perp/\mu_\perp$ is large.

Consider the case when $\mu_\perp^i \gg \mu_\perp^e$, $\Delta T_e \approx 0$, and $(\Phi_w-\Phi_f)/T_e \approx 1.5$. Equations (30) and (22) predict that the change in applied bias across the electrode,

$\Delta(\Phi_w-\Phi_f)/T_e$, is of order unity when the radial extent of the electrode, Δr, exceeds

$$\Delta r \gtrsim 1.3 \frac{\lambda_0 T_e \mu_\perp^i}{D_\perp} . \qquad (31)$$

Assuming for the moment that the magnitudes of the phenomenological mobility and diffusion coefficients satisfy an Einstein-like relationship, $D_\perp \sim T \mu_\perp$, Eq. (31) would require the biased limiters to be segmented into a series of electrodes with radial widths no larger than the "unperturbed" density e-folding distance, λ_0. Otherwise, the ratio of λ/λ_0 may not be maintained over the full electrode width into the scrape-off layer. (The density reduction shown in section 3 would then be overly "optimistic" for the cases when $\delta > \lambda_0$.)

The dimensionless ratio of phenomenological "diffusion" arising from potential gradients versus "diffusion" arising from density gradients, $\Lambda = T \mu_\perp/D_\perp$, is therefore very important for assessing the viability of the EBSOL technique. Should the plasma exhibit transport properties such that Λ is much smaller than of order unity, the EBSOL technique may be difficult to implement, since many closely spaced and independently biased electrodes may be required.

4.2 Choice of Model for Phenomenological Cross-Field Mobility

Mobility-like transport, namely, transport that depends in some way on the local electric field, arises across the magnetic field from processes which exchange momentum with **ExB** drifting plasma species. Such processes include: (1) collisions of the **ExB** drifting species with a species that is not drifting or drifting at a different speed (a neutral species or a species drifting at a different velocity due to finite gyroradius effects, for example) and/or (2) cross-field momentum transport in a sheared flow. The latter processes include turbulent shear viscosity (through correlated fluctuations).

The rate of local momentum exchange may be most simply viewed as an equivalent "drag force", **F**, on the **ExB** drifting species. The result is a species-dependent **FxB** drift which is in the direction of $\pm$**E**. For the case of momentum exchange mechanisms which are independent of flow shear (such as in neutral collisions), the resultant **FxB** drift is proportional to the local electric field strength and can be simply expressed as an effective cross-field mobility as in Eqs. (1) and (2). However, since cross-field momentum exchange rates generally depend on flow shear, the appropriate "phenomenological value" for mobility may exhibit a more complicated dependence on the spatial variation of Φ, among other things (such as the details of the plasma turbulence and the dependence of the turbulence

on local plasma parameters). Predictions from the simplified non-ambipolar transport model presented above should therefore be treated with appropriate caution. Nevertheless, in spite of its inherent shortcomings, the model does allow a rough estimate of the overall transport modification that can occur from an applied bias. Given that the current level of quantitative understanding of turbulent transport processes in edge plasmas is poor at best, more elaborate forms for the phenomenological diffusion and mobility terms in Eqs. (1)-(2) and the further complexity that they introduce are difficult to justify.

4.3 Comments on SOL Transport Analysis with Finite $\mu_\perp$

The dependence of the density e-folding length on both the diffusion coefficient and the local wall bias as suggested by Eqs. (18)-(20) has a number of important implications for the interpretation of experimental data taken in a tokamak SOL. Typically, cross-field transport in a tokamak SOL is assumed to be governed solely by the density gradient through a "diffusive" transport process. The effective value of the cross-field diffusion coefficient is usually estimated from an equation of the form of Eq. (21). However, Eqs. (18)-(20) suggest that by accounting for mobility-like transport processes, this definition for the effective diffusion coefficient may be in error. (This is reminiscent of the neglect of Simon's short-circuit effect [14] during early transport experiments in weakly ionized plasmas.) Diffusion coefficients estimated from this "incorrect" formula may be an order of magnitude to high or too low than the "actual" diffusion coefficient, depending on the wall potential relative to the local floating potential. The consequences of this oversight can be important; Density e-folding length asymmetries reported in some tokamaks may, in part, be a manifestation of a local variation of the plasma potential relative to the potential of the limiter, divertor, or wall that intercepts the magnetic field lines; When scaling SOL diffusion coefficients with core plasma conditions, one may need to account for changes in plasma potential profiles across the SOL.

The density profile in the SOL may also exhibit a characteristic e-folding length that is a function of radius, i.e. a non-exponential profile. In the absence of mobility-like transport (or a local ionization source), it may be considered that the effective diffusion coefficient varies as a function of radius. However, by allowing for mobility-like transport processes, it may be alternatively considered that the effective diffusion coefficient is relatively independent of radius but that the quantity $(\Phi_W-\Phi_f)/T_e$ changes with radius (due to $T_e(r)$, for example).

Finally, it should be pointed out that the mobility terms in Eqs.(1) and (2) may be viewed as convection or "pinch" terms. It is recognized that inward pinches play a role in the central plasma for both hydrogenic and impurity species. One may similarly presume that mobility-like terms may play a role for impurity transport

in the SOL plasma, particularly since it is expected from scaling arguments that $\mu_\perp^z >> \mu_\perp^i$.

4.4 The Need for Experimental Data on $\Phi(r)$ and $\mu_\perp$

In order to assess the relative merit of the EBSOL scheme, one needs to assume some value for the dimensionless parameter, $\Lambda = T\mu_\perp/D_\perp$. In partially ionized plasmas, this ratio may be roughly estimated by considering that mobility primarily arises from neutral collisions and that the diffusion coefficient is typically on the order of Bohm. However, in fully ionized turbulent plasmas, it is not obvious what value Λ assumes. The Einstein relationship ($\Lambda = 1$) may not apply. At the same time the limit of $\Lambda = 0$ does not apply since it would then be possible to impose very large electric fields resulting in **ExB** flows of arbitrarily high shear and velocities that could exceed the ion sound speed.

Clearly a need exists for experimental data on phenomenological values for Λ in fully ionized, turbulent boundary layer plasmas. At least the plasma potential profile should be recorded along with the density profile in a tokamak scrape-off layer. As a first-cut approach to estimating Λ, one may then use a transport model that includes mobility-like transport effects such as the crude model outlined in section 2.

5. SUMMARY

An Electrostatic Barrier Scrape-Off Layer (EBSOL) is considered as a technique which may be used to reduce the bombarding flux of plasma onto RF antenna components. The EBSOL may be particularly well suited for controlling the plasma density profile in the vicinity of an RF antenna where the competing requirements of a high plasma density near the antenna (for good coupling) yet a low plasma density at the antenna surface (for low sputtering) coexist. The technique can be incorporated into existing RF antenna designs to protect the Faraday shield with some relatively minor modifications. A dynamic control of the plasma density at the Faraday shield may also be beneficial from the point of view of diagnosis and experimentation.

A simplified non-ambipolar transport model is developed for an EBSOL. Turbulent cross-field ion and electron transport is assumed to be modelled by phenomenological coefficients of diffusion and mobility. The model yields a rough estimate of the density profile modification that can be expected when an electrical bias is applied. The model predicts that the influence of an applied bias on the local density e-folding length depends only on the relative magnitudes of cross-field ion

and electron mobilities and is explicitly independent of the magnetic field strength, the cross-field diffusion coefficient, and the mechanisms that determine the phenomenological values of $\mu_\perp^i$ and $\mu_\perp^e$ when $\mu_\perp^i >> \mu_\perp^e$.

The transport model is used to assemble graphs of the reduction in density e-folding length, reduction in density at an antenna's Faraday shield, total bias current, and peak heat flux on the biased limiter segments as a function of applied bias. It is shown that the characteristic density e-folding length in front of the Faraday shield may be reduced by up to a factor of ~5 with positive bias potentials on the order of ~3 T_e. However, such biases can be accompanied by at factor of ~10 increase in the peak heat flux to the biased surfaces. Moderate biases of ~1.5 T_e result in a more acceptable factor of ~2.5 increase in the heat peak flux and also yield a factor of ~2 reduction in the density e-folding length. In all cases, the model indicates that an order of magnitude or more reduction in the ion sputtering rate on the Faraday shield may be achievable.

As a specific example of this technique, an EBSOL arrangement that might be employed to protect the Faraday shield of an Alcator C-MOD ICRF antenna structure is considered. Acceptable values of bias potential, current, and peak power flux to the protection limiters are estimated to yield an order of magnitude or more reduction in the ion sputtering rate on the Faraday shield in this tokamak.

Finally, assumptions and limitations of the simplified non-ambipolar transport model are discussed. The transport parameter Λ ($= T\,\mu_\perp/D_\perp$) is shown to be important for assessing the practical viability of the EBSOL technique. In the cases where Λ is small, the biased limiters may need to be segmented in radius in order to apply a wall bias that follows the radial plasma potential variation. It is noted that tokamak SOL transport analysis can be refined by incorporating mobility-like transport processes in models for the edge plasma. It is pointed out that experimental data on cross-field mobility in a turbulent plasma boundary layer is lacking. In particular, typical values for the dimensionless ratio of phenomenological "diffusion" arising from potential gradients versus "diffusion" arising from density gradients, Λ, are not established for a fully ionized, turbulent boundary layer plasma. The need for measurements of both plasma potential and plasma density profiles in the tokamak SOL is encouraged both for assessing the viability of techniques such as an EBSOL and for developing a more complete understanding of tokamak SOL transport.

ACKNOWLEDGEMENTS

The author gratefully acknowledges Prof. R.W. Conn, R. Lehmer, Dr. L. Schmitz, G. Tynan, and co-workers at the Institute for Plasma and Fusion Research, UCLA, for their support and encouragement of the author's experimental studies at the PISCES facility on the use of an EBSOL to control boundary layer fluxes in a tokamak. Discussions with Dr. S. Golovalto, Prof. I.H. Hutchinson, Dr. B. Lipschultz, and Dr. Y. Takase on using an EBSOL for protecting the Faraday shield of an ICRF antenna in C-MOD are also greatly appreciated. This work is supported by the U.S. Department of Energy.

REFERENCES

[1] Cohen, S.A., Bernabei, S., Budny, R., Chu, T.K., Colestock, P., Hinnov, E., Hooke, W., Hosea, J., Hwang, D., Jobes, F., Manos, D., Motley, R., Ruzic, D., Stevens, J., Stratton, B., Suckewer, S., Von Goeler, S., Wilson, R., "Plasma-Materials Interactions during RF Experiments in Tokamaks", J. Nucl. Mater. **128&129** (1984) 280.

[2] Stratton, B.C., Moos, H.W., Hodge, W.L., Suckewer, S., Hosea, J.C., Hulse, R.A., Hwang, D.Q., Wilson, J.R., "Changes in Impurity Radiation during ICRF Heating of PLT Tokamak Plasmas", Nucl. Fusion **24** (1984) 767.

[3] Manning, H.L., Terry, J.L., Lipschultz, B., LaBombard, B., Blackwell, B.D., Fiore, C.L., Foord, M.E., Marmar, E.S., Moody, J.D., Parker, R.R., Porkolab, M., Rice, J.E., "Impurity Generation during ICRF Heating Experiments on Alcator C", Nucl. Fusion **26** (1986) 1665.

[4] Caughman, J.B.O., Ruzic, D.N., Hoffman, D.J., "The Effects of Radio Frequency Waves on the Sputtering of Ion Cyclotron Resonance Heating Antenna Faraday Shields", J. Vac. Sci. Technol. **A5** (1987) 2301.

[5] Stangeby, P.C., McCracken, G.M., a review to be submitted to Nuclear Fusion.

[6] Taylor, R.J., James, B.W., Jin, S.X., Keller, L., Lee, P.S.C., Luhmann Jr., N.C., Morales, G.J., Oren, L., Park, H., Peebles, W.A., Talmadge, S., Yu, C.X., "Particle Transport Due to ICRF Waves and Radial Electric Fields in Tokamaks", Proceedings of 9th IAEA Conference on Plasma Physics and Controlled Nuclear Fusion Research, Baltimore, Vol. III (1982) p. 251.

[7] Oren, L., Keller, F., Schwirzke, F., Talmadge, S., Taylor, R.J., "Influence Exerted by the Plasma Edge Potential on Recycling, Sputtering and Impurity Accumulation", J. Nucl. Mater. **111&112** (1982) 34.

[8] Phillips, P.E., Wootton, A.J., Rowan, W.L., Ritz, Ch.P., Rhodes, T.L., Bengtson, R.D., Hodge, W.L., Durst, R.D., McCool, S.C., Richards, B., Gentle, K.W., Brower, D.L., Peebles, W.A., Luhmann Jr., N.C., Schooch, P., Forster, J.C., Hickok, R.L., Evans, T.E., "Biased Limiter Experiments on TEXT", J. Nucl. Mater. **145-147** (1987) 807.

[9] Shimada, M. et al., "Limiter Biasing Experiments in PBX Tokamak", Bull. Amer. Phys. Soc. **30** (1985) 1439.

[10] Conn. R.W, et al.., "ALT-I Pump Limiter Behavior and Edge Plasma Flows During Biasing and ICRF Heating in the TEXTOR Tokamak", Proceedings of 11th IAEA Conference on Plasma Physics and Controlled Nuclear Fusion Research, Kyoto, Vol. I (1987) p. 249.

[11] LaBombard, B., Lehmer, R., Chung, K.S., Conn, R.W., Hirooka, Y., Nygren, R.E., "Biased SOL Simulation Experiments in PISCES: An Investigation of the Use of Electrical Bias to Modify Tokamak SOL Transport", Bull. Amer. Phys. Soc. **33** (1988) 2103.

[12] LaBombard, B., Conn, R.W., Tynan, G., "An Electrostatic Barrier Scrape-off Layer for Control of Core Plasma Effluxes in Tokamaks", submitted for publication in Plasma Physics and Controlled Fusion.

[13] LaBombard, B., Conn, R.W., "Analysis of an m=1 Electrostatic Barrier Scrape-off Layer as a Technique for Reducing and Controlling the Particle and Energy Losses on the Large Major Radius Edge of a Tokamak", UCLA IPFR Report No. PPG-1186 (1988).

[14] Simon, A., "Ambipolar Diffusion in a Magnetic Field", Phys. Rev. **98** (1955) 317.

[15] Stangeby, P.C., "Plasma Sheath Transmission Factors for Tokamak Edge Plasmas", Phys. Fluids **27** (1984) 682.

[16] LaBombard, B., Lipschultz, B., "Poloidal Asymmetries in the Scrape-off Layer Plasma of the Alcator C Tokamak", Nucl. Fusion **27** (1987) 81.

Figure Captions

Fig. 1 - Model geometry for parallel and perpendicular transport in a biased scrape-off layer (BSOL). Limiter/divertor plates are biased to a potential, Φ_w, which may be different than the floating potential, Φ_f.

Fig. 2 - Concept of using a local EBSOL to reduce plasma sputtering of an RF antenna's Faraday shield. Limiter segments intercepting magnetic field lines in front of the Faraday shield are biased positive to reduce the density e-folding length relative to its no-bias value.

Fig. 3 - Relative reductions in plasma density at Faraday shield and density e-folding length in local EBSOL as a function of positive bias applied to limiter segments with (a) $\mu_\perp^i >> \mu_\perp^e$ and (b) $\mu_\perp^i = \mu_\perp^e$. The case of $\mu_\perp^i << \mu_\perp^e$ yields no density profile modification.

Fig. 4 - Normalized peak power flux and total bias current on the biased limiter segments as a function of applied voltage. (See text for description of units.)

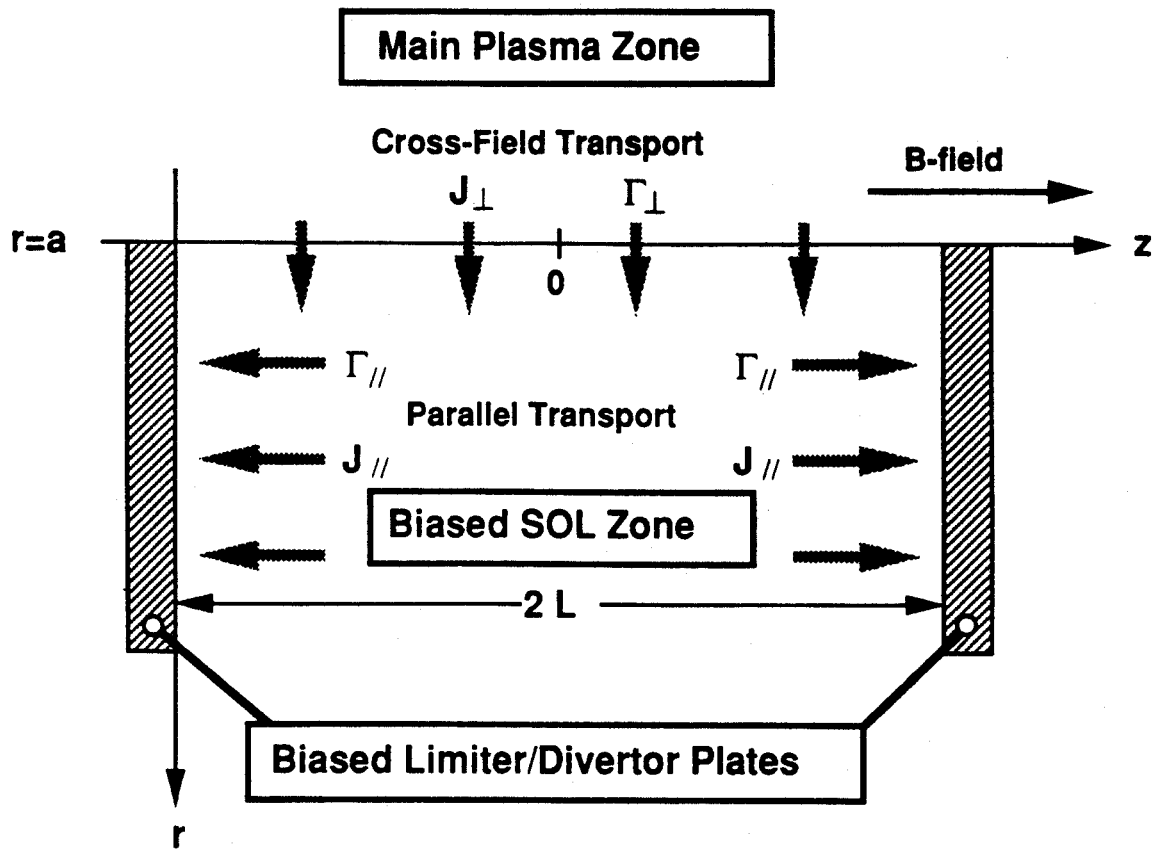
Main Plasma Zone
Cross-Field Transport
B-field
J⊥
Γ⊥
r=a
z
0
Γ//
Γ//
Parallel Transport
J //
J //
Biased SOL Zone
2 L
Biased Limiter/Divertor Plates
r

FIGURE 1

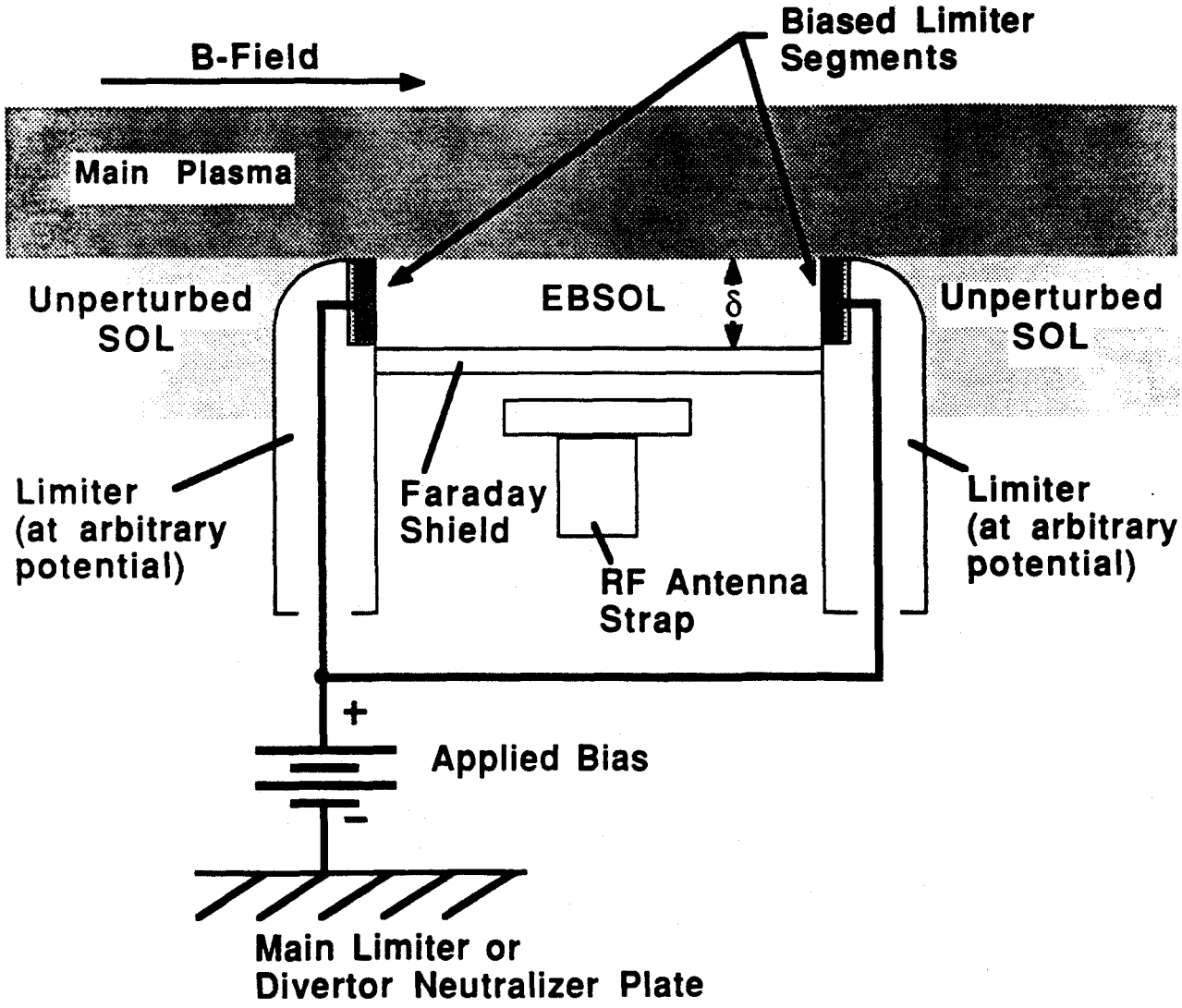
B-Field
Biased Limiter Segments
Main Plasma
Unperturbed SOL
EBSOL
δ
Unperturbed SOL
Limiter (at arbitrary potential)
Faraday Shield
RF Antenna Strap
Limiter (at arbitrary potential)
+
Applied Bias
−
Main Limiter or Divertor Neutralizer Plate

FIGURE 2

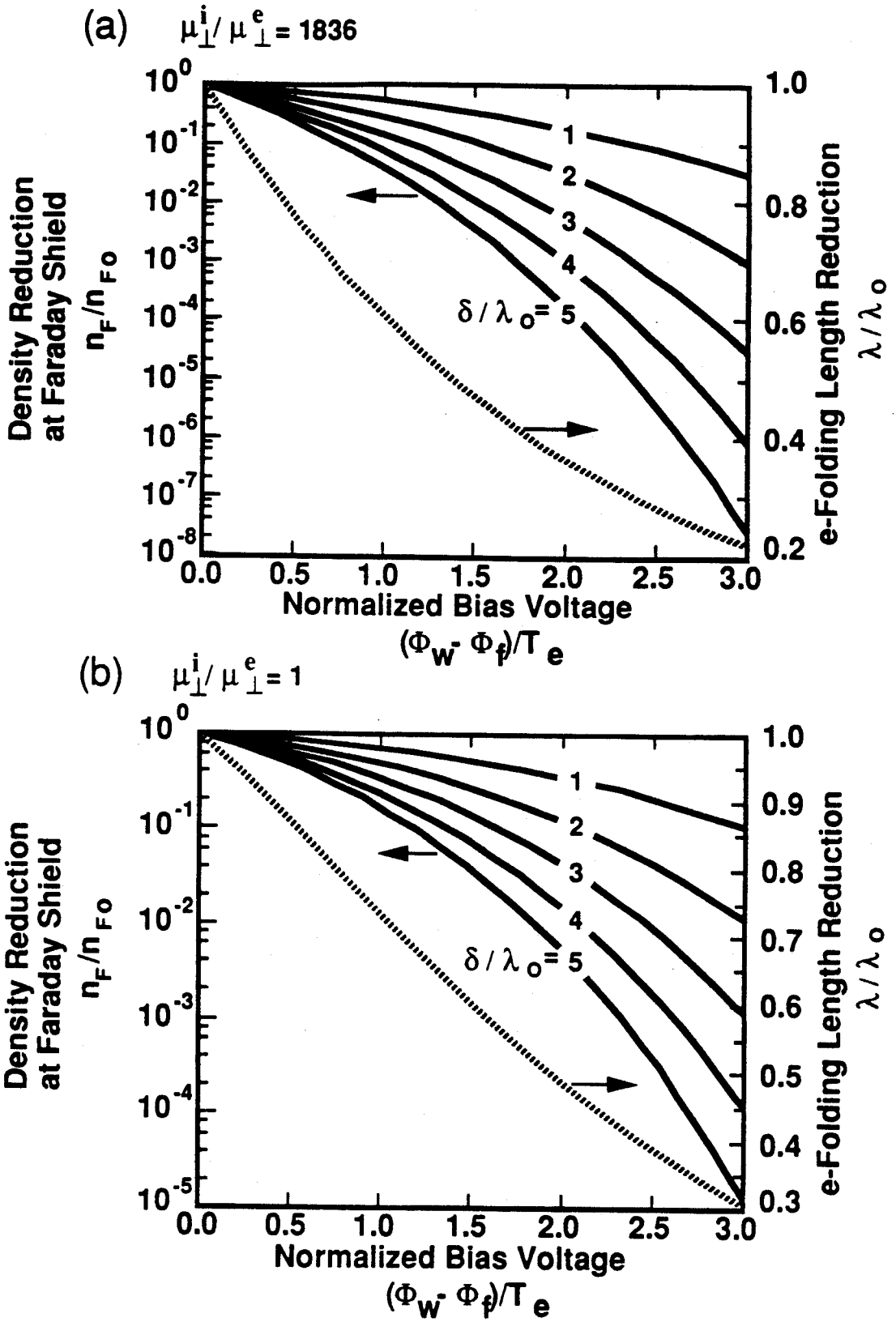
(a) $\mu^i_\perp / \mu^e_\perp = 1836$
Density Reduction at Faraday Shield
n_F/n_{Fo}
e-Folding Length Reduction
λ/λ_o
$\delta/\lambda_o = 5$
Normalized Bias Voltage
$(\Phi_w - \Phi_f)/T_e$
(b) $\mu^i_\perp / \mu^e_\perp = 1$
Density Reduction at Faraday Shield
n_F/n_{Fo}
e-Folding Length Reduction
λ/λ_o
$\delta/\lambda_o = 5$
Normalized Bias Voltage
$(\Phi_w - \Phi_f)/T_e$

FIGURE 3

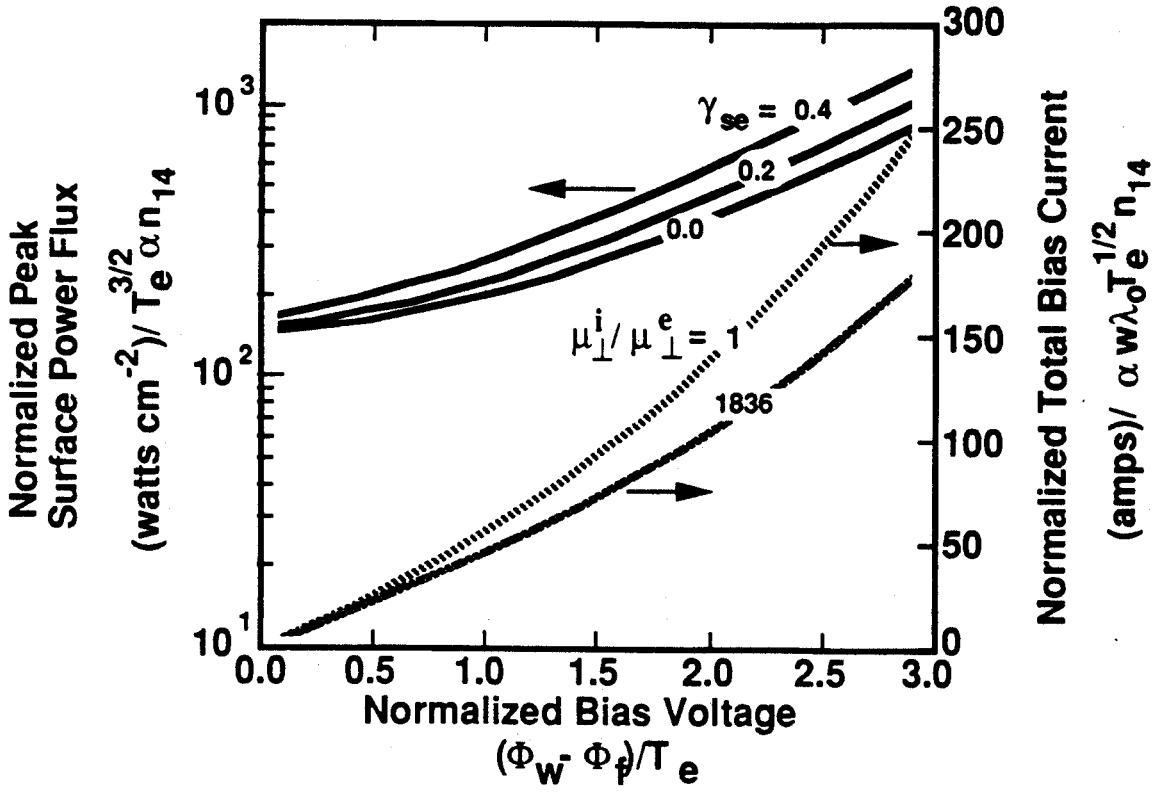
Normalized Peak
Surface Power Flux
(watts cm^{-2})/ $T_e^{3/2} \alpha n_{14}$
10^3
10^2
10^1
γ_{se} = 0.4
0.2
0.0
$\mu^i_\perp / \mu^e_\perp = 1$
1836
300
250
200
150
100
50
0
Normalized Total Bias Current
(amps)/ $\alpha w \lambda_o T_e^{1/2} n_{14}$
0.0
0.5
1.0
1.5
2.0
2.5
3.0
Normalized Bias Voltage
$(\Phi_w - \Phi_f)/T_e$

FIGURE 4

Table 1 - Estimated Plasma Density Reduction at the Faraday Shield of a RF Antenna in the Alcator C-MOD Tokamak using an EBSOL

Bias Voltage	Recess Distance of Faraday Shield		Density at Faraday Shield, $n_F(cm^{-3})$		Density Reduction Factor, n_F/n_{Fo}		Total Bias Current I_b (amps)		Peak Power Flux P_p (kW/ cm^2)		
$(\Phi_W - \Phi_f)/T_e$	δ (cm)	δ/λ_o	$\mu_\perp^i >> \mu_\perp^e$	$\mu_\perp^i \approx \mu_\perp^e$	$\mu_\perp^i >> \mu_\perp^e$	$\mu_\perp^i \approx \mu_\perp^e$	$\mu_\perp^i >> \mu_\perp^e$	$\mu_\perp^i \approx \mu_\perp^e$	γ_{se}= 0.0	0.2	0.4
0	0.24	2	6.8×10^{12}	6.8×10^{12}	1	1	0	0	3.2	3.4	3.6
	0.36	3	2.5×10^{12}	2.5×10^{12}	1	1					
	0.48	4	9.2×10^{11}	9.2×10^{11}	1	1					
1.0	0.24	2	1.8×10^{12}	3.3×10^{12}	0.27	0.48	310	375	4.4	5.0	6.0
	0.36	3	3.6×10^{11}	8.4×10^{11}	0.14	0.34					
	0.48	4	6.8×10^{10}	2.1×10^{11}	0.075	0.23					
1.5	0.24	2	7.2×10^{11}	1.8×10^{12}	0.11	0.27	490	625	5.9	6.9	8.6
	0.36	3	8.7×10^{10}	3.5×10^{11}	0.035	0.14					
	0.48	4	1.1×10^{10}	6.7×10^{10}	0.011	0.073					
2.0	0.24	2	2.2×10^{11}	8.3×10^{11}	0.032	0.12	700	930	8.5	10.2	13.1
	0.36	3	1.4×10^{10}	1.1×10^{11}	0.0058	0.043					
	0.48	4	9.5×10^{8}	1.4×10^{10}	0.0010	0.015					

Plasma Conditions: $D_\perp = 10D_{Bohm}$ $T_e = 20$ eV $T_i = 20$ eV

$n_o = 5\times10^{13}\ cm^{-3}$ $L = 10$ cm $\alpha = 0.5$ $w = 50$ cm

$\lambda_o = 0.12$ cm $B = 7$ T $\rho_i/\lambda_o = 0.05$